Many-body effects in semiconductor lasers

Weng W. Chow
Sandia National Labs
Albuquerque, NM 87185-0350

ABSTRACT

A microscopic theory, that is based on the coupled Maxwell-semiconductor-Bloch equations, is used to investigate the effects of many-body Coulomb interactions in semiconductor laser devices. This paper describes two examples where the many-body effects play important roles. Experimental data supporting the theoretical results are presented.

1 INTRODUCTION

A population inversion is created in a semiconductor laser when there are electrons in the conduction band and holes in the valence band. Being charged particles, the electrons and holes interact with one another. These interactions are called many-body interactions because a laser typically has very high electron and hole densities. The effects of many-body Coulomb interactions include plasma screening, a carrier density dependence of bandgap energy commonly referred to as bandgap renormalization, excitonic or Coulombic enhancement of optical transitions, relaxation of intraband carrier populations to quasi-equilibrium distributions, and dephasing of electron-hole polarizations.[1]

This paper presents evidence of many-body effects in semiconductor laser devices. We describe two examples: one involving a class of microcavity lasers called vertical-cavity surface-emitting lasers, and the second involving short-wavelength lasers operating with wide-bandgap materials.

2 MANY-BODY THEORY

This section gives an overview of the theory used in our study. Detailed descriptions may be found in Refs. (1) and (2).

The working equations are derived using the following many-body Hamiltonian,

$$H = H_{kin} + H_C + H_{dipole} \quad , \tag{1}$$

where the kinetic energy is

$$H_{kin} = \sum_{\vec{k}} (\varepsilon_{c,\vec{k}} a^{\dagger}_{\vec{k}} a_{\vec{k}} + \varepsilon_{h,\vec{k}} b^{\dagger}_{\vec{k}} b_{\vec{k}}) \quad , \tag{2}$$

the Coulomb interaction is

$$H_C = \frac{1}{2} \sum_{\vec{k},\vec{k}',\vec{q}\neq 0} V_q (a^{\dagger}_{\vec{k}+\vec{q}} a^{\dagger}_{\vec{k}'-\vec{q}} a_{\vec{k}'} a_{\vec{k}} + b^{\dagger}_{\vec{k}+\vec{q}} b^{\dagger}_{\vec{k}'-\vec{q}} b_{\vec{k}'} b_{\vec{k}} - 2 a^{\dagger}_{\vec{k}+\vec{q}} b^{\dagger}_{\vec{k}'-\vec{q}} b_{\vec{k}'} a_{\vec{k}}) \quad , \tag{3}$$

and the interaction of the carrier with the laser field, $E(z,t)$, gives

$$H_{dipole} = -\sum_{\vec{k}} [\mu_{\vec{k}} a^{\dagger}_{\vec{k}} b^{\dagger}_{-\vec{k}} + \mu^{*}_{\vec{k}} b_{-\vec{k}} a_{\vec{k}}] E(z,t) \quad . \tag{4}$$

We use a second quantized notation, where $a_{\vec{k}}$, $a^{\dagger}_{\vec{k}}$ and $b_{\vec{k}}$, $b^{\dagger}_{\vec{k}}$ are the annihilation and creation operations for the electrons and holes, respectively, to account for the quantum statistics of the electrons and holes. The bandstructure information is contained in the single particle energies, $\varepsilon_{c,\vec{k}}$ and $\varepsilon_{h,\vec{k}}$, and in the dipole matrix element, $\mu_{\vec{k}}$. In Eq. (3), the terms simply describe the Coulomb repulsion between electrons and between holes, and the Coulomb attraction between electrons and holes.

Working in the Hiesenberg picture and using a semiclassical laser theory to incorporate Maxwell's equations into the derivation lead to the Maxwell-semiconductor-Bloch equations (MSBE).[3–6] These equations describe the interaction between a laser field and a semiconductor medium under the influence of many-body Coulomb interactions. They consist of two coupled sets of equations: the semiconductor-Bloch-equations (SBE) and the reduced wave equation (RWE). The latter,

$$\frac{\partial \mathcal{E}(\eta,\xi)}{\partial \xi} = \frac{i\mu_0 \omega_0^2}{k_0 V} \sum_{\vec{q}} \mu_{\vec{q}} P_{\vec{q}}(\eta,\xi) \quad , \tag{5}$$

describes the propagation of the light field envelope $\mathcal{E}$ in a semiconductor medium, where μ_0 is the permeability, ω_0 and k_0 are the optical carrier frequency and wavevector, V is the volume of

the active region, $\eta = t - z/c$ and $\xi = z$ are the retarded time and space coordinates obtained by using a traveling frame at the group velocity c of the pulse, and the summation is over all electron-hole momenta. The source term on the right hand side is determined by the total polarization $\sum_{\vec{q}} \mu_{\vec{q}} P_{\vec{q}}$. where each polarization function $P_{\vec{q}}$ with electron wave number $\vec{q}$ obeys the SBE:

$$\frac{\partial P_{\vec{q}}}{\partial \eta} = -i\left(\omega_{\vec{q}} - \omega_0\right) P_{\vec{q}} - i\Omega_{\vec{q}}(f^e_{\vec{q}} + f^h_{\vec{q}} - 1) + \frac{\partial P_{\vec{q}}}{\partial \eta}|_{coll} \tag{6}$$

and

$$\frac{\partial f^{e/h}_{\vec{q}}}{\partial \eta} = (iP^{\star}_{\vec{q}}\Omega_{\vec{q}} + c.c.) + \frac{\partial f^{e/h}_{\vec{q}}}{\partial \eta}|_{coll} \quad . \tag{7}$$

In the above equations, the Rabi frequency of the light,

$$\Omega_{\vec{q}} = \hbar^{-1}(\mu_{\vec{q}} E + \sum_{\vec{q}'} V_{\vec{q}-\vec{q}'} P_{\vec{q}'}) \tag{8}$$

is renormalized by Coulomb many-body terms, where $V_{\vec{q}}$ is the screened Coulomb potential in Fourier space. Also, $\hbar\omega_{\vec{q}} = \hbar\omega_{\vec{q},0} + \Delta\varepsilon_{SX} + \Delta\varepsilon_{CH}$ is the renormalized transition energy, where $\hbar\omega_{\vec{q},0}$ is the single particle transition energy, $\Delta\varepsilon_{SX}$ and $\Delta\varepsilon_{CH}$ are the screened exchange and Coulomb-hole contributions to the bandgap renormalization. Equation (7) is the equation of motion for $f^{e/h}_{\vec{q}}$, which is the electron/hole population distribution. The collision terms, $\frac{\partial P_{\vec{q}}}{\partial \eta}|_{coll}$ and $\frac{\partial f^{e/h}_{\vec{q}}}{\partial \eta}|_{coll}$ are due to intraband carrier-carrier collisions, which tend to drive the nonequilibrium population distributions into quasi-equilibrium Fermi-functions and yield optical dephasing. In our treatment they are linearized in the relaxation rate approximation with time constants of $50fs$ to$100fs$.[7]

Equations (5) through (7) allow one to study the nonlinear optical response of a semiconductor in the presence of many-body Coulomb interactions. A general problem involves solving the MSBE for a broad-band laser pulse propagating in some semiconductor structure. Fourier-transforming the optical field afterwards allows us to, for example, extract the gain or absorption at each frequency. Under most lasing conditions and for many semiconductor material systems, the MSBE may be simplified to yield direct expressions for gain and carrier-induced refractive index (see Chap. 5 in Ref. (2)).

3 VERTICAL-CAVITY SURFACE-EMITTING LASERS

The first example of many-body interactions affecting the performance of a laser device involves the vertical-cavity surface-emitting laser (VCSEL).[8] This laser is characterized by a very short ($\approx \lambda$) resonator that is perpendicular to the plane of the active region. The resonator is made with very high reflectivity distributed Bragg reflectors (DBRs). Due to the short high-Q resonator, there is often only one optical mode within the spectral gain region, resulting in single longitudinal mode operation, which is highly desirable for some applications. On the other hand, having only one resonator mode under the gain curve means that the laser threshold current is very sensitive to the alignment of this resonance in relation to gain peak.

Figure 1 shows typical dependence of threshold current on VCSEL wavelength. The points are experimental data taken with $GaInP$ quantum well VCSELs from the same wafer.[9] The wafer was not rotated during growth, so that there is sufficient variation in layer thicknesses or compositions to provide VCSELs with a range of lasing wavelength. One clearly sees that there is an optimal wavelength where the threshold current is minimum and that the threshold current increases rapidly with deviation from this wavelength. The curve in Fig. 1 is obtained using the many-body theory. If many-body effects are neglected (i.e. free-carrier theory), the theoretical curve will be red shifted by roughly $20nm$.

The agreement between many-body theory and experiment has been shown to be quite general.[10] Plotted in the Fig. 2 are data from five experimental devices with different heterostructure compositions, and with quantum well widths varying from $6nm$ to $10nm$. Except for one $10nm$ quantum well device, the theory predicts the experimental measurements very well. The discrepancy with the cw measurement for the $6nm$ quantum well device is likely due to the reduction in bandgap energy with increasing temperature. Our calculations are performed for $T = 300K$, while the laser gain medium is most likely at an elevated temperature during cw operation. The difference in behavior between the two supposedly similar 10nm devices, and the theory's inability to explain the difference point to the fact that further work remains for the theoretical analysis and the experiment. On the other hand, considering the wide range of experimental laser structures, the agreement between theory and experiment is very satisfactory, especially since all theoretical curves are computed using the same bulk material parameters obtained from the literature.[11–14] No attempt is made to optimize the input parameters to provide a better fit.

The temperature dependence of the threshold current also shows many-body effects.[15] The cavity-gain alignment, which we have just shown to be very critical to achieving a low threshold current, can be maintained only within a small temperature range. This is because the gain spectrum and the cavity resonances have different temperature dependences. The result is a temperature dependence of the cavity-gain alignment, which plays an important role in the sensitivity of a VCSEL output to temperature variations. Figure 3 shows experimental data (hollow squares) for the lasing current threshold of an $InGaAs$ VCSEL as a function of temperature. Details on the experimental device are described elsewhere.[16] The dashed curve is the best fit

possible using the free-carrier theory. We see that the free-carrier theory significantly overestimates the temperature sensitivity of the threshold current at low temperatures. The agreement with experiment when the many-body effects are taken into account (solid curve) is significantly better.

Further studies using the many-body theory has shown VCSEL temperature stability may improve when operating away from the wavelength that gives the minimum threshold. Even greater improvement is possible by making use of the higher lying quantum well subband transitions.[17]

4 WIDE-BANDGAP LASERS

The second example, where many-body interactions affect laser properties, involves short-wavelength semiconductor lasers. These lasers are based on wide-bandgap group-III nitrides[18,19] and II-VI compounds[20–22] and they operate in the blue-green and potentially in the ultraviolet wavelength regions. Since these compounds are characterized by large exciton binding energies, many-body Coulomb effects significantly influence their optical properties.[23–25]

Using the MSBE to simulate an amplifier experiment for determining gain in a GaN gain medium, we obtained the gain/absorption spectra at $T = 300K$, as shown in Fig.4a. The results show a pronounced excitonic absorption peak at low density. This excitonic absorption decreases in amplitude with increasing carrier density and disappears with the appearance of gain at high density. The disappearance of the bound excitonic state is due to the filling of the electron and hole states and to more effective plasma screening. On the other hand, Fig. 4b shows that at the lower temperature of $T = 77K$, the gain spectra takes on a very different character. The absorption peak remains even at the high densities where gain is present, which nicely illustrates the effect of excitonic enhancement.

Figure 5 shows the gain spectra at $T = 300K$ for a II-VI $ZnCdSe$ quantum well structure. Comparison of the free-carrier and many-body results shows significant energy shifts due to bandgap renormalization, and noticeable reshaping of the spectra due to Coulomb enhancement. For the spectrum showing a peak gain of $1000cm^{-1}$, which is typical material threshold gain for quantum well lasers, the theory predicts a peak gain energy that is approximately $30meV$ redshifted from the absorption edge. This agrees very well with experiments performed at room temperature,[22] suggesting that at high temperatures, the electron-hole plasma, under the influence of strong many-body Coulomb interactions, may be responsible for the laser gain in II-VI materials.

Finally, Fig. 6 shows the antiguiding,[26] R at gain peak as a function of peak gain, for the ZnCdSe quantum well. The antiguiding or linewidth enhancement factor is a measure of the change in carrier-induced refractive index relative to a corresponding change in gain. Compared to that of a GaAs quantum well, R for the II-VI compound is significantly smaller. More interesting, the theory predicts the occurrence of negative values for the antiguiding factor. The

dashed curve shows that both of these properties are due to many-body interactions.

5 SUMMARY

We use a microscopic laser theory, that is based on the Maxwell-semiconductor-Bloch equations in the screened Hartree-Fock approximation, to investigate the many-body Coulomb effects in semiconductor laser devices. For the vertical-cavity surface-emitting lasers and the wide-bandgap lasers, which are two areas currently experiencing considerable research and developmental activities, many-body Coulomb interactions are shown to significantly affect the laser properties. Experimental results supporting this conclusion are presented.

6 ACKNOWLEDGMENTS

Parts of this work is performed in collaboration with M. Crawford, R. Schneider, Jr., S. Corzine, S. Koch and A. Knorr. The work was supported by the U.S. Department of Energy through contract No. DE-AC04-94DP85000. The author also gratefully acknowledges the hospitality and support from Philipps-Universitaet, Marburg, during his visit there.

7 REFERENCES

[1] H. Haug and S. W. Koch, *Quantum Theory of the Optical and Electronic Properties of Semiconductors*, 3rd ed. (World Scientific, Singapore, 1994).

[2] W. W. Chow, S. W. Koch and M. Sargent III, *Semiconductor-Laser Physics* (Springer Verlag, Berlin, 1994).

[3] W. Schäfer and K. Henneberger, Phys. Stat. Sol. B 159, **59** (1990).

[4] A. Knorr, R. Binder, E. M. Wright and S. W. Koch, Opt. Lett. **18**, 1538 (1993).

[5] A. Knorr, R. Binder, M. Lindberg and S. W. Koch, Phys. Rev. A **46**, 7179 (1992).

[6] R. Binder and S.W. Koch, *Nonequilibrium Semiconductor Dynamics*, Progr. Quantum Electron. (1995).

[7] R. Binder, D. Scott, A. Paul, M. Lindberg, K. Henneberger and S. W. Koch, Phys. Rev. B **45**, 1107 (1992).

[8] Special issue on semiconductor lasers, IEEE J. Quantum Electron. **QE-27**, 1476 (1991).

[9] M. Hagerott Crawford, R.P. Schneider Jr., K.D. Choquette, K.L. Lear, S.P. Kilcoyne, and J.J. Figiel, 'High efficiency AlGaInP-based 660-680 nm VCSELs', Electron. Lett. (submitted).

[10] W.W. Chow, R.P. Schneider Jr., J.A. Lott, and K.D. Choquette, Appl. Phys. Lett **65**, 135 (1994).

[11] *Landolt-Bornstein, New Series, Vol. 17, Semiconductor subvol. a, Physics of Group IV elements and III-V Compounds* (Springer-Verlag, Berlin, Heidelberg, New York, 1982).

[12] G.B. Stringfellow, J. Appl. Phys. **43**, 3455 (1972).

[13] M. D. Dawson and G. Duggan, Phys. Rev. B, 47, 12598 (1993).

[14] S. Adachi, *Physical Properties of III-V Semiconductor Compunds*, John Wiley & Sons, New York (1992).

[15] W.W. Chow, S.W. Corzine, D.B. Young, and L.A. Coldren, 'Many-body effects in the temperature dependence of threshold in a VCSEL', Appl. Phys. Lett. (to be published).

[16] D.B. Young, S.W. Corzine, F.H. Peters, J.W. Scott, B.J. Thibeault and L.A. Coldren, Conf. Proc. LEOS '92, 546, Nov. 16-19 (1992) Boston, MA.

[17] W.W. Chow, M.D. Choquette and P.L. Gourley, 'Effects of quantum well subbandstructure on the temperature stability of VCSELs', Appl. Phys. Lett. (to be published).

[18] S. Strite, M. E. Lin and H. Morkoc, Thin Solid Films **231**, 197 (1993).

[19] X. H. Yang, T. J. Schmidt, W. Shan J. J. Song and B. Goldenberg, Appl. Phys. Lett. **66**, 1 (1995).

[20] A. V. Nurmikko, R. L. Gunshor and M. Kobazyashi, J. Vac. Sci. Technol. B 10, 2056 (1992)

[21] M. A. Haase, J. Qiu, J. M. Depuydt and H. Cheng, Appl. Phys. Lett. 59, 1272 (1991)

[22] J. Ding, M. Hagerott, T. Ishihara, H. Jeon and A. V. Nurmikko, Phy. Rev. B47, 10528 (1993).

[23] S. W. Koch, H. Haug, G. Schneider, W. Bohnert and C. Klingshirn, Phys. Stat. Sol. (b) **89**, 431 (1978).

[24] W. W. Chow, A. Knorr and S. W. Koch, 'Theory of laser gain in Group III-nitrides,' Appl. Phys. Lett. (submitted).

[25] W. W. Chow and S. W. Koch, Many-body Coulomb effects in room-temperature II-VI quantum well semiconductor lasers,'Appl. Phys. Lett. (to be published).

[26] P. Kirby, A. Goodwin, G. Thompson and P. Selway, IEEE J. Quantum Electron. **QE-13**, 705 (1977).

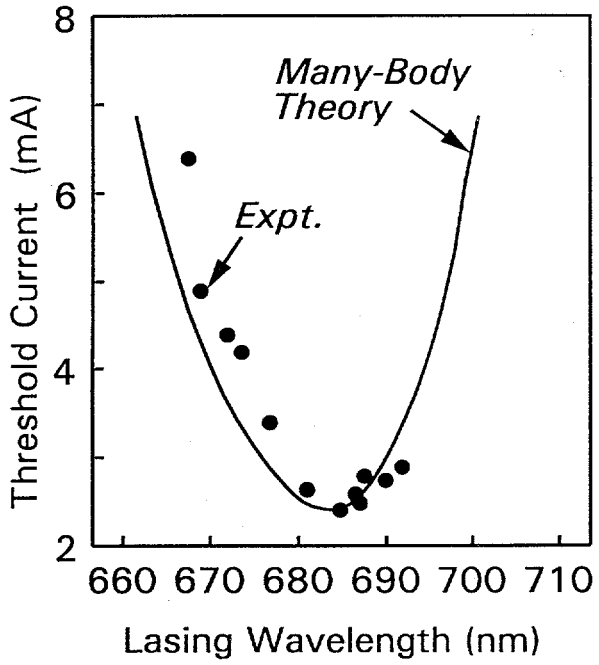

Fig. 1. InGaP quantum well VCSEL threshold current vs. wavelength at 300K.

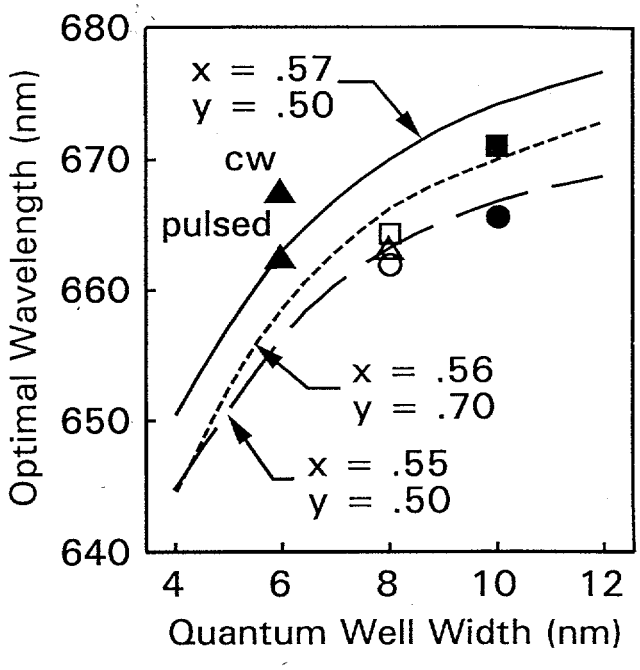

Fig. 2. Optimal laser wavelength vs. quantum well width for $In_xGa_{1-x}P$-$In_{0.5}(Al_yGa_{1-y})_{0.5}P$ at 300K. The experimental results for 6nm, 8nm and 10nm qw widths are to be compared with the solid, long-dashed and short-dashed curves, respectively..

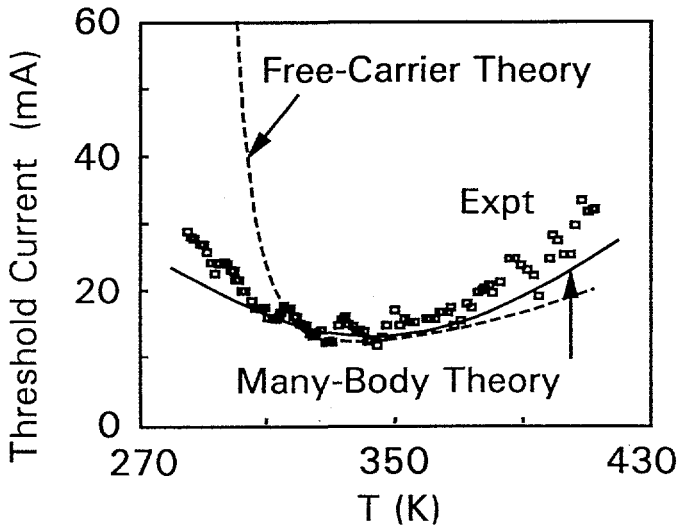

Fig. 3. VCSEL threshold current vs. temperature.

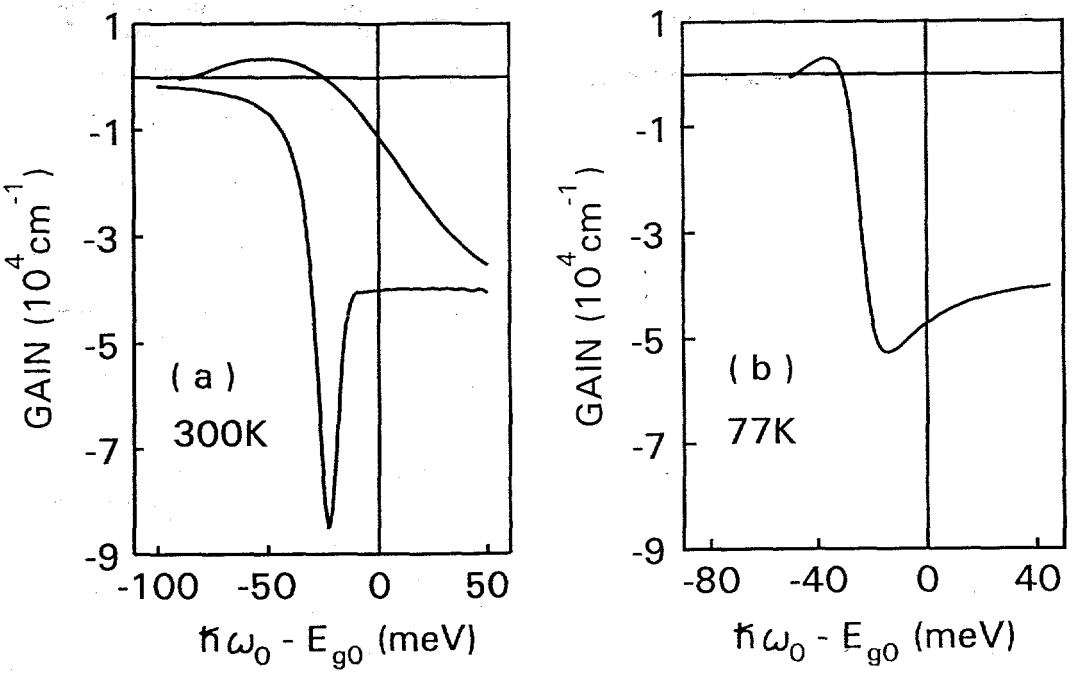

Fig. 4. Computed gain/absorption spectra at (a) T=300K and (b) T=77K, for bulk GaN. The carrier densities are (a) N=10^{17}cm^{-3} and 1.2x10^{19}cm^{-3}, and (b) N=2.2x10^{18}cm^{-3}. The photon energy is referenced to the unexcited bulk material bandgap energy.

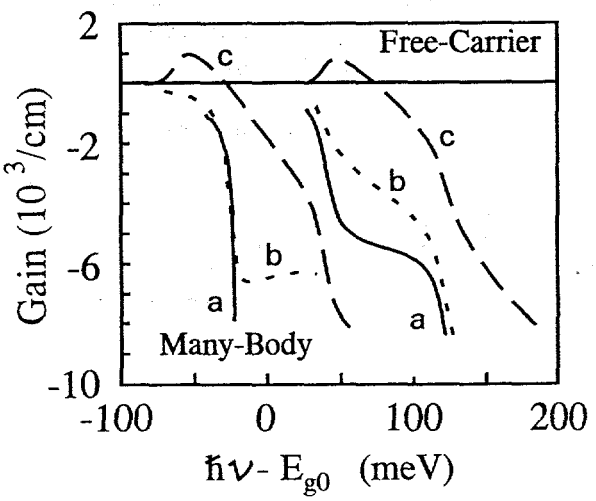

Fig. 5. Computed gain spectra at T = 300K for 8nm $Zn_{0.8}Cd_{0.2}Se$ quantum well. The carrier densities are N = (a) 10^{11}cm^{-2}, (b) 1.2 x 10^{12}cm^{-2} and (c) 4 x 10^{12}cm^{-2}. The photon energy is referenced to the unexcited bulk material bandgap energy.

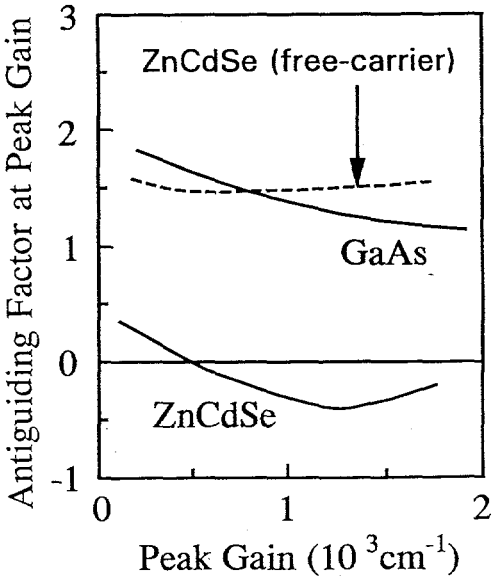

Fig. 6. Antiguiding factor at gain peak vs. peak gain.